Inorg. Chem. **2006**, *45*, 94–101

Interaction of 2- and 4-Mercaptopyridine with Pentacyanoferrates and Gold Nanoparticles†

Fábio Souza Nunes,‡ Leonardo Da Silva Bonifácio,§ Koiti Araki,§ and Henrique Eisi Toma*,§

Instituto de Química, Universidade de São Paulo, C.P. 26077, 05513-970 São Paulo, São Paulo, Brazil, and Departamento de Química, Universidade Federal do Paraná, C.P. 19081, 81531-990, Curitiba, PR, Brazil

Received July 25, 2005

2-Mercapto- and 4-mercaptopyridine (2- and 4MPy) react with the $[Fe(CN)_5(H_2O)]^{3-}$ complex, forming the S-coordinated $[Fe(CN)_5(2MPy)]^{3-}$ and the N-coordinated $[Fe(CN)_5(4MPy)]^{3-}$ complexes. The rates of formation and dissociation of the $[Fe^{II}(CN)_5(2MPy)]^{3-}$ complex were determined as $k_f = 294$ dm^3 mol^{-1} s^{-1} and $k_d = 0.019$ s^{-1} by means of stopped-flow technique. The equilibrium constants for the iron(II) and -(III) species were calculated as $K_f^{II} = 1.5 \times 10^4$ mol^{-1} dm^3 and $K_f^{III} = 1.3 \times 10^6$ mol^{-1} dm^3, in comparison with 2.6×10^5 and 3.4×10^4 mol^{-1} dm^3, respectively, for the 4MPy isomer. In the presence of gold nanoparticles, both 2- and 4MPy can displace the stabilizing citrate species, leading to substantial aggregation in aqueous solution, as deduced from the surface-enhanced Raman spectroscopy effect and from the decay of the 520-nm plasmon band accompanied by the rise of the characteristic exciton band at 650 nm. The $[Fe(CN)_5(4MPy)]^{3-}$ complex promotes strong stabilization of the gold nanoparticles by interacting through the S atom. On the other hand, the labile $[Fe(CN)_5(2MPy)]^{3-}$ complex induces aggregation, delivering the 2MPy ligand to the gold nanoparticles.

Introduction

Stabilization of gold nanoparticles can be carried out based on a coordination chemistry approach, using suitable multifunctional bridging ligands such as mercaptopyridine, capable of simultaneously binding transition-metal ions and gold nanoparticles (Figure 1). The main attractive point of this approach is the possibility of incorporating the characteristics of the metal complexes into the modified nanoparticles, allowing their controlled charge stabilization while imparting new optical, chemical, electrochemical, and catalytic properties.

The interaction of 2- and 4-mercaptopyridine (2- and 4MPy) with gold nanoparticles has recently been investigated by Fourier transform infrared (FTIR) spectroscopy in the solid state, revealing significant differences in their aggregation behavior.[1] 2MPy leads to stable nanoparticles, while 4MPy-coated nanoparticles exhibit a strong tendency to form 3D aggregates, because of cross-linking between sulfur groups on neighboring particles. The binding of 4MPy to pentacyanometalate complexes has also been reported,[2] including their immobilization onto gold surfaces and their redox mediator activity for electrochemically probing cyto-

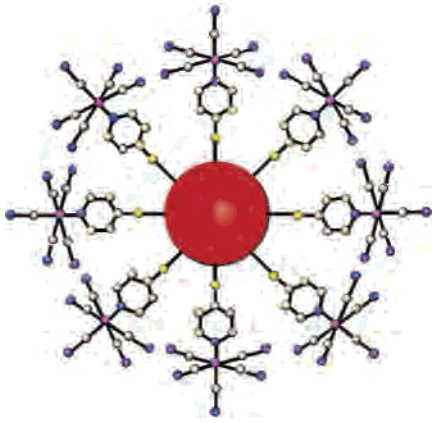

Figure 1. Stabilization of a gold nanoparticle by means of a $[Fe(CN)_5L]^{3-}$ complex.

† Dedicated to Henry Taube (1915−2005).

* To whom correspondence should be addressed. E-mail: henetoma@iq.usp.br.

‡ Universidade Federal do Paraná.

§ Universidade de São Paulo.

(1) Zhang, H.-L.; Evans, S. D.; Henderson, J. R.; Miles, R. E.; Shen, T. *J. Phys. Chem. B* **2003**, *107*, 6087.

(2) Diogenes, I. C. N.; de Souza, J. R.; de Carvalho, I. M. M.; Temperini, M. L. A.; Tanaka, A. A.; Moreira, I. D. S. *J. Chem. Soc., Dalton Trans*. **2003**, 2231. Corio, P.; Andrade, G. F. S.; Diogenes, I. C. N.; Moreira, I. S.; Nart, F. C.; Temperini, M. L A. *J. Electroanal. Chem.* **2002**, *520*, 40.

10.1021/ic0512429 CCC: $33.50
Published on Web 12/09/2005

chrome *c*. However, the interaction of gold nanoparticles with the 2MPy- and 4MPy-pentacyanoferrate(II) complexes has never been reported before.

Pentacyanoferrate(II) ions have been used to probe the binding affinity of specific donor atoms toward iron.[3] This is justified because the cyanides in $[Fe(CN)_5]^{3-}$ are substitution inert; therefore, only one coordinating site is available for interacting with a specific donor atom of a multifunctional ligand (L).[3] On the other hand, the chemical properties of the products, $[Fe(CN)_5L]^{3-}$, are strongly dependent on the nature of L. For instance, pentacyanoferrate(II) ions show a high affinity for *N*-heterocycles,[3,4] amino acids,[5] and S-containing ligands, such as sulfoxides,[6] thioethers,[7] and thioamides.[8]

There is extensive information gathered about ligand substitution reactions of pentacyanoferrate(II) complexes,[9] including the $[Fe(CN)_5(4MPy)]^{3-}$ species[2] but not the $[Fe(CN)_5(2MPy)]^{3-}$ isomer. Such information is quite relevant for the use of pentacyanoferrate(II) complexes in the stabilization of gold nanoparticles. For this reason, a detailed investigation of the kinetics and redox properties of the $[Fe(CN)_5(2MPy)]^{3-}$ complex has also been carried out in this work.

Experimental Section

Materials. $Na_3[Fe(CN)_5NH_3]\cdot 3H_2O$ was prepared from sodium nitroprusside as described in the literature.[10] The ligands 2- and 4-pyridinethiol were obtained from Aldrich. The $[Fe(CN)_5L]^{3-}$ complexes (L = 2- or 4MPy) were prepared by combining equimolar amounts of 4×10^{-3} mol dm^{-3} solutions of $[Fe(CN)_5NH_3]^{3-}$ and L. All other chemicals were of analytical-grade quality and were used as supplied.

Gold nanoparticles were obtained according to the following procedure:[11] 100 mL of a 0.01% solution of $AuCl_3$ was heated to boiling under vigorous stirring, and 3 mL of a 1% sodium citrate solution was added. The color of the solution turned to violet and burgundy within about 1 min. After that, the solution was cooled, continuing stirring for about 20 min. A characteristic absorption band at 520 nm was observed in the electronic spectrum, consistent with the average size of 20 nm for the nanoparticles, measured by light scattering techniques.

Physical Measurements. The electronic spectra were recorded on a Hewlett-Packard model 8453 diode-array spectrophotometer. Raman spectra in the region of 350−2000 cm^{-1} were recorded on an In Photonics portable instrument, equipped with a 785-nm laser for excitation. Additional Raman spectra in the 300−2500-cm^{-1} region were kindly provided by the Molecular Spectroscopy Laboratory (Universidade de São Paulo) using a Renishaw Spectrometer System 3000 and 632.8-nm excitation radiation from a He−Ne laser (Spectra Physics).

The kinetics of formation was investigated with a Durrum model D-110 stopped-flow apparatus, equipped with a Kel-F flow system. The aquapentacyanoferrate(II) complex was generated at concentrations smaller than 10^{-4} mol dm^{-3} by dissolving the appropriate amount of $Na_3[Fe(CN)_5NH_3]\cdot 3H_2O$ into argon-saturated water. The kinetics was investigated in the presence of dimethyl sulfoxide (DMSO), which has a strong affinity for pentacyanoferrate,[4] allowing the dissociation reactions to be easily monitored. The rates of substitution were studied at four different concentrations of 2MPy (3.9×10^{-3}−2.0×10^{-2} mol dm^{-3}), keeping the DMSO concentration constant (5.0×10^{-3} mol dm^{-3}).

The cyclic voltammetry measurements were carried out with a Princeton Applied Research model 173 potentiostat and a model 175 universal programmer. A gold disk electrode was employed for the measurements at an ionic concentration of 0.1 mol dm^{-3} in KCl. A Ag/AgCl (1 mol dm^{-3} KCl) with a Luggin capillary and a platinum wire were used as reference and auxiliary electrodes, respectively. Typical experiments were conducted with a 5×10^{-3} mol dm^{-3} complex concentration.

The spectroelectrochemical experiments were carried out using a HP8452A and a PARC-173 potentiostat. A three-electrode system was designed for a rectangular quartz cell of 0.025-cm internal optical path length. A gold minigrid was used as the transparent working electrode, in the presence of a small Ag/AgCl (KCl 1 mol dm^{-3}) reference electrode and of a platinum auxiliary electrode. All experiments were done at 25 °C, under semi-infinite diffusion conditions.

The electronic spectra of gold nanoparticles and their aggregates were recorded in a successive scanning mode, after the addition of very small amounts of 2MPy, 4MPy, $[Fe(CN)_5(2MPy)]^{3-}$, or $[Fe(CN)_5(4MPy)]^{3-}$ to 3 cm^3 of gold nanoparticles. The final concentration of the ligand was typically in the range of 6×10^{-8} mol dm^{-3}. For the measurement of the surface-enhanced Raman spectroscopy (SERS) effect, 3×10^{-4} mol dm^{-3} solutions of such species have been employed.

Results and Discussion

Complex Formation between 2- and 4MPy and $[Fe(CN)_5]^{3-}$. The aquapentacyanoferrate(II) ion reacts rapidly with 2MPy, producing an orange complex that absorbs at 450 nm, with $\epsilon = 2400$ dm^3 mol^{-1} cm^{-1}. The cyclic voltammogram of this solution shows a reversible wave with $E_{1/2} = 272$ mV vs standard hydrogen electrode (SHE), assigned to the Fe^{II}/Fe^{III} couple. Typical spectroelectrochemical changes can be seen in Figure 1. As the applied potential is varied from −200 to +150 mV (vs Ag/AgCl), the intensity of the 450-nm band decreases, producing a green solution that absorbs at 670 nm. On the basis of the Nernst equation, the formal redox potential, $E°$, was calculated as 275 mV vs SHE, coinciding with the $E_{1/2}$ values obtained by cyclic voltammetry.

(3) Toma, H. E.; Malin, J. M. *Inorg. Chem.* **1973**, *12*, 1039.
(4) Toma, H. E.; Malin, J. M.; Giesbrecht, E. *Inorg. Chem.* **1973**, *12*, 2084.
(5) Borges, S. S. S.; Coelho, A. L.; Moreira, I. S.; Araújo, M. A. B. *Polyhedron* **1994**, *13*, 1015. Baraldo, L. M.; Forlano, P. F.; Parise, A. R.; Slep, L. D.; Olabe, J. A. *Coord. Chem. Rev.* **2001**, *219*, 881.
(6) Toma, H. E.; Martins, J. M. *J. Chem. Soc., Dalton Trans*. **1978**, 1610. Toma, H. E.; Batista, A. A.; Gray, H. B. *J. Am. Chem. Soc*. **1982**, *104*, 7509.
(7) Toma, H. E.; Serrasqueiro, R. M.; Rocha, R. C.; Demets, G. J. F.; Winnischofer, H.; Araki, K.; Ribeiro, P. E. A.; Donnici, C. L. *J. Photochem. Photobiol. A* **2000**, *135*, 185.
(8) Toma, H. E.; Takasugi, M. S. *Polyhedron* **1982**, *1*, 429.
(9) Toma, H. E.; Malin, J. M. *Inorg. Chem.* **1973**, *12*, 2080. Maciejowska, I.; Stasicka, Z.; Stochel, G.; van Eldik, R. J. *Chem. Soc., Dalton Trans.* **1999**, 3643. Stochel, G.; van Eldik, R. *Inorg. Chim. Acta* **1991**, *190*, 55. Alshehri, S.; Burguess, J.; van Eldik, R.; Hubbard, C. D. *Inorg. Chim. Acta* **1995**, *240*, 305. Lin, C. L.; Hung, K.; Yeh, A. *Inorg. Chem.* **1999**, *38*, 411. Chen, C. N.; Wu, M. C.; Yeh, A.; Tsai, T. Y. R. *Inorg. Chim. Acta* **1998**, *267*, 81. Toma, H. E.; Chavez-Gil, T. E. *Spectrosc. Lett.* **1999**, *32*, 963. Norris, P. R.; Harper, P. L. S.; Pratt, J. M. *J. Chem. Soc., Dalton. Trans*. **1997**, 2505. Almaraz, A. E.; Gentil, L. A.; Baraldo, L. M.; Olabe, J. A. *Inorg. Chem.* **1996**, *35*, 7718.
(10) Brauer, G. *Handbook of Preparative Inorganic Chemistry*, 2nd ed.; Academic Press: New York, 1965; Vol. 2, p 1511.
(11) Turkevitch, J.; Stevenson, P. C.; Hilier, J. *Discuss. Faraday Soc.* **1951**, *11*, 55.

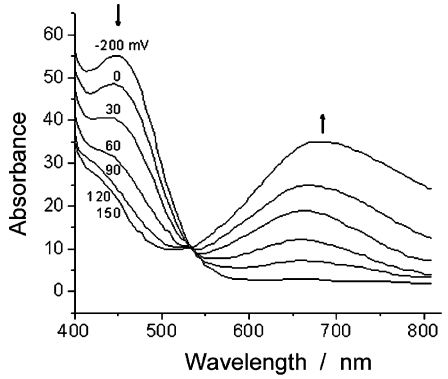

Figure 2. Absorption spectra of $[Fe(CN)_5(2MPy)]^{3-/2-}$ at different applied potentials (E vs Ag/AgCl, 1 mol dm^{-3} KCl) and pH 5.72.

The pK_a values of 2MPy, obtained from spectrophotometric titrations, were pK_a^1 = 1.79 and pK_a^2 = 9.72, contrasting with those of typical pyridine species and supporting the conclusion that the molecule exists in solution as the thione tautomer:

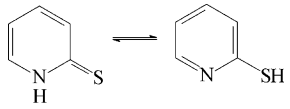

thione thiol

The N atom in both tautomeric forms is not available for coordination because of protonation or the steric hindrance from the vicinal SH group. Therefore, 2MPy can only bind to the $[Fe(CN)_5]^{3-}$ ion via the S atom. Thione ligands are known to form stable complexes with pentacyanoferrate(II) and -(III) species, displaying strong metal-to-ligand or ligand-to-metal charge-transfer bands in the visible, respectively.[8] The absorption band at 450 nm for the $[Fe(CN)_5(2MPy)]^{3-}$ complex is consistent with an iron(d_π) → 2MPy(p_π*) charge-transfer transition involving the iron(II) thione chromophore.[8] In addition, low-energy bands, e.g., above 600 nm, are not observed in the spectra of pentacyanoferrate(III) complexes containing N-coordinated pyridines,[3] while they are prominent in the spectra of pentacyanoferrate(III) complexes containing S-donor ligands[12] such as thiourea (595 nm), 2-mercaptobenzoxazole (706 nm), 3-mercapto-1,2,4-triazole (693 nm), mercaptosuccinate (700 nm), diethyldithiocarbamate (785 nm), and 2-mercaptopyridine-*N*-oxide (shpyNO; 736 nm), being ascribed to a $p_\pi(S) \rightarrow d_\pi(Fe^{III})$ charge-transfer transition. Therefore, the lowest energy band at 700 nm in the spectroelectrochemical data shown in Figure 2 support the iron coordination via the S atom, presumably from the thione group.

The reaction of the $[Fe(CN)_5(H_2O)]^{3-}$ complex with 2MPy, yielding $[Fe^{II}(CN)_5(2MPy)]^{3-}$, proceeds very fast and can be monitored by the stopped-flow technique, following the increase of the 450-nm band with time. By the addition of DMSO as a $[Fe(CN)_5(H_2O)]^{3-}$ scavenger, a competitive scheme (eq 1) can be explored, allowing a simultaneous evaluation of the formation and dissociation kinetic constants.

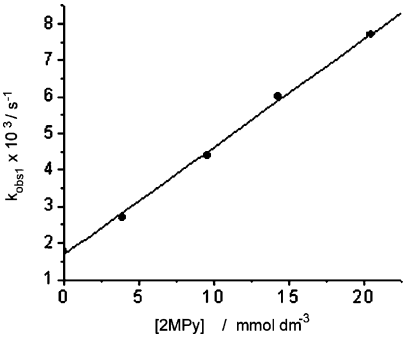

Figure 3. Plot of k_{obs1} vs ligand concentration for the formation of $[Fe^{II}(CN)_5(2MPy)]^{3-}$ at [DMSO] = 5 × 10^{-3} mol dm^{-3} and 25 °C.

$$[Fe(CN)_5(H_2O)]^{3-} + 2MPy \underset{k_{-2MPy}}{\overset{k_{2MPy}}{\rightleftharpoons}} [Fe(CN)_5(2MPy)]^{3-} + H_2O$$

$$[Fe(CN)_5(H_2O)]^{3-} + DMSO \xrightarrow{k_{DMSO}} [Fe(CN)_5(DMSO)]^{3-} + H_2O \quad (1)$$

In this case, a rapid reaction was observed, corresponding to the parallel formation of $[Fe(CN)_5(2MPy)]^{3-}$ (λ_{max} = 450 nm) and $[Fe(CN)_5(DMSO)]^{3-}$ (colorless), followed by a second, slow reaction, converting the less stable $[Fe(CN)_5(2MPy)]^{3-}$ species into the thermodynamically stable $[Fe(CN)_5(DMSO)]^{3-}$ product, leading to the complete decay of the 450-nm band.

The parallel formation reaction proceeded according to a first-order kinetics. In this case, the observed rate constant can be expressed by eq 2, exhibiting the following values:

$$k_{obs1} = k_{DMSO}[DMSO] + k_{2MPy}[2MPy] \quad (2)$$

k_{obs1} = 2.7, 4.4, 6.0, and 7.7 s^{-1} for [MPy] = 3.9, 9.6, 14.3, and 20.5 × 10^{-3} mol dm^{-3}, respectively. From the linear plot of k_{obs} vs [2MPy], shown in Figure 3, it is possible to extract k_{2MPy} = 294 dm^3 mol^{-1} s^{-1} and k_{DMSO} = 336 dm^3 mol^{-1} s^{-1}.

The formation rate constants, k_f^{II}, are similar to those previously described for the substitution in $[Fe(CN)_5(H_2O)]^{3-}$ (240−400 dm^3 mol^{-1} s^{-1}), reflecting the typical dissociative mechanism involved.[3,9]

Conversion of the orange $[Fe^{II}(CN)_5(2MPy)]^{3-}$ complex into the colorless $[Fe^{II}(CN)_5(DMSO)]^{3-}$ product proceeds more slowly, according to well-defined and reproducible first-order kinetics. The corresponding observed rate constants can be fitted by eq 3.[3]

$$k_{obs2} = \frac{k_{-2MPy}k_{DMSO}[DMSO]}{k_{2MPy}[2MPy] + k_{DMSO}[DMSO]} \quad (3)$$

$$\frac{1}{k_{obs2}} \frac{k_{2MPy}[2MPy]}{k_{-2MPy}k_{DMSO}[DMSO]} + \frac{1}{k_{-2MPy}} \quad (4)$$

(12) Gale, R.; McCaffery, A. J. *J. Chem. Soc., Dalton Trans.* **1973**, 1344. Luiz, J. B.; Leigh, G. J.; Nunes, F. S. *Polyhedron* **2002**, *21*, 2137. Baran, Y.; Ülgen, A. *Int. J. Chem. Kinet.* **1998**, *30*, 415. Szachowski, K.; Oszajca, J.; Stochel, G.; Stasicka, Z. *J. Chem. Soc., Dalton Trans.* **1999**, 2353. Böll, J. B.; Andrade, F. M.; Evans, D. J.; Friederman, G.; Mangrich, A. S.; Hasegawa, T.; Nunes, F. S. *J. Braz. Chem. Soc.* **2004**, *15*, 10.

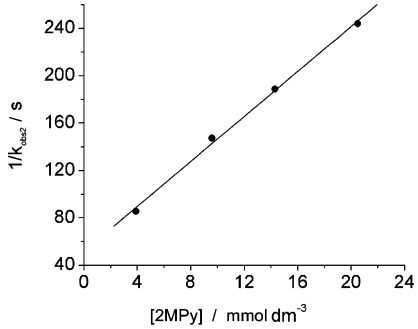

Figure 4. Reciprocal plot of k_{obs2} for the dissociation reaction of $[Fe^{II}(CN)_5(2MPy)]^{3-}$ at [DMSO] = 5×10^{-3} mol dm^{-3} and 25 °C.

The values of k_{obs2} obtained from concentrations of 2MPy = 3.9, 9.6, 14.3, and 20.5×10^{-3} mol dm^{-3} were 11.7, 6.8, 5.3, and 4.1×10^{-3} s^{-1}, respectively. From the reciprocal plot (eq 4 shown in Figure 4), the dissociation constant k_{-2MPy} was determined as 0.019 s^{-1}, leading to an equilibrium constant $K^{II} = k_{2MPy}/k_{-2MPy} = 1.5 \times 10^4$ dm^3 mol^{-1}.

The stability constant K_f^{II} indicates that 2MPy behaves as a moderate π-acceptor ligand, capable of stabilizing the reduced form of the pentacyanoferrate complex.

The stability constant for the corresponding iron(III) species, $K_f^{III} = 6.1 \times 10^5$ dm^3 mol^{-1}, can be calculated from the electrochemical potentials, according to the redox cycle

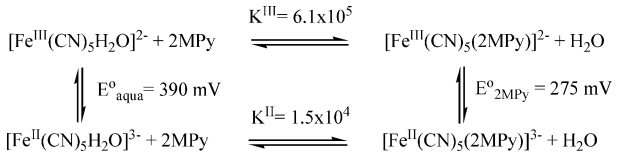

where

$$K^{III} = K^{II}\left\{\exp\left[\frac{nF}{RT}(E^\circ_{2MPy} - E^\circ_{aqua})\right]\right\}^{-1} \qquad (5)$$

The fact that K_f^{III} is 1 order of magnitude higher than K_f^{II} is consistent with the strong π-donor character of the C=S group. This dual stabilization behavior, for both oxidation states, has also been observed for histidine, imidazole, and 2-mercaptobenzoxazole.[6,12]

In the case of the 4MPy ligand, the corresponding $[Fe(CN)_5(4MPy)]^{3-}$ has been previously reported in the literature.[2] The complex exhibits a characteristic absorption band at 405 nm, ascribed to a metal-to-ligand charge-transfer transition. UV−visible and Raman spectroscopy support the coordination of 4MPy through the N atom, in contrast with the 2MPy isomer. Its redox potential has been measured by cyclic voltammetry as 442 mV (vs SHE). The dissociation kinetics has also been studied in the presence of a large excess of DMSO, yielding a dissociation rate constant $k_{-4MPy} = 1.1 \times 10^{-3}$ s^{-1}, about 17 times smaller in comparison to that for the 2MPy isomer. Assuming a similar formation rate constant (which is characteristic of the $[Fe(CN)_5(H_2O)]^{3-}$ species), the equilibrium constant for the $[Fe(CN)_5(4MPy)]^{3-}$ complex can be calculated as $K = 294/0.0011 = 2.6 \times 10^5$ mol^{-1} dm^3.

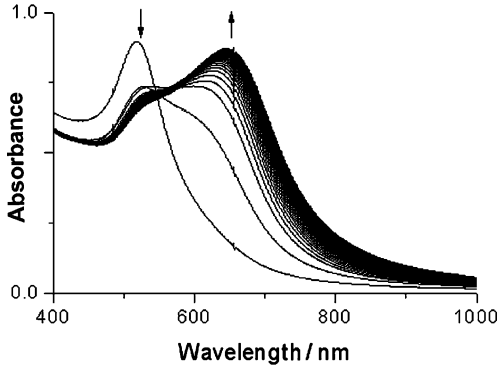

Figure 5. Successive spectra (time interval = 120 s) of a citrate-stabilized gold nanoparticle solution, after the addition of 2MPy in a final concentration of 5×10^{-6} mol dm^{-3}.

By comparing the k_{-L}^{II} values for the $[Fe^{II}(CN)_5L]^{2-}$ complexes, one can establish the following order of increasing lability (Table 1): DMSO (7.5×10^{-5} s^{-1}) < pyrazine (4.2×10^{-4} s^{-1}) < py, 4MPy (1.1×10^{-3} s^{-1}) < 2MPy (1.9×10^{-2} s^{-1}), reflecting the relative importance of back-bonding stabilization in these iron(II) compounds.

Interaction of 2MPy and Gold Nanoparticles. The binding of 2MPy to gold nanoparticles has been previously investigated in the solid state, using FTIR spectroscopy.[1] Starting from citrate-stabilized gold nanoparticles, one can see that the initial plasmon absorption band at 520 nm undergoes a rapid initial decrease, associated with the binding of 2MPy, followed by the rise of a new band at 650 nm (Figure 5). With an increase in the 2MPy concentration, the 650-nm band is dramatically enhanced while the initial band at 520 nm becomes only slightly smaller. This new band accounts for the aggregation of the gold nanoparticles,

Table 1. Kinetic and Thermodynamic Data for $[Fe(CN)_5L]^{2-/3-}$ Complexes[a]

L	donor group	k_d^{II}, s^{-1} at 25 °C	k_f^{II}, mol^{-1} s^{-1} at 25 °C	K_f^{II}, dm^3 mol^{-1}	K_f^{III}, dm^3 mol^{-1}	E°_L[b]	ref
DMSO	S=O	7.5×10^{-5}	2.4×10^2	4.9×10^6	3.7×10^{-2}	850	4, 6
pyrazine	C=N	4.2×10^{-4}	3.80×10^2	1.9×10^6 [c]	1.7×10^3	550	3, 5, 6
isonicotinamide	C=N	7.3×10^{-4}	2.95×10^2	8.2×10^5 [c]	5.2×10^3	500	3, 5, 6
pyridine	C=N	1.1×10^{-3}	3.65×10^2	4.6×10^5 [c]	9.4×10^3	470	3, 5, 6
4MPy[c]	C=N	1.1×10^{-3}	$\sim 2.9 \times 10^2$ [d]	$\sim 2.6 \times 10^5$	$\sim 3.4 \times 10^4$	442	2
histidine	C=N	5.3×10^{-4}	3.20×10^2	5.9×10^5	1.1×10^6	355	6
imidazole	C=N	1.3×10^{-3}	2.4×10^2	1.8×10^5	5.8×10^5	340	6
2MPy[c]	C=S	1.7×10^{-2}	2.9×10^2	1.5×10^4	1.3×10^6	275	*e*
bzoxsh[f]	C=S	3.7×10^{-4}	2.9×10^2	7.8×10^5	8.6×10^8	190	12
mtr[g]	C=S	4.6×10^{-4}	3.0	1.5×10^4	[h]	[h]	12
1,4-dithiane	R−S−R	5.6×10^{-4}	[h]	[h]	[h]	[h]	12

[a] The entries are on the order of decreasing reduction potentials, E°_L. [b] mV vs SHE; the values refer to the $Fe^{III} + e^- \rightarrow Fe^{II}$ reversible process. [c] 4-Mercapto- and 2-mercaptopyridine. [d] Assumed as the same value for 2MPy. [e] This work. [f] 2-Mercaptobenzoxazole. [g] 3-Mercapto-1,2,4-triazole. [h] Not determined.

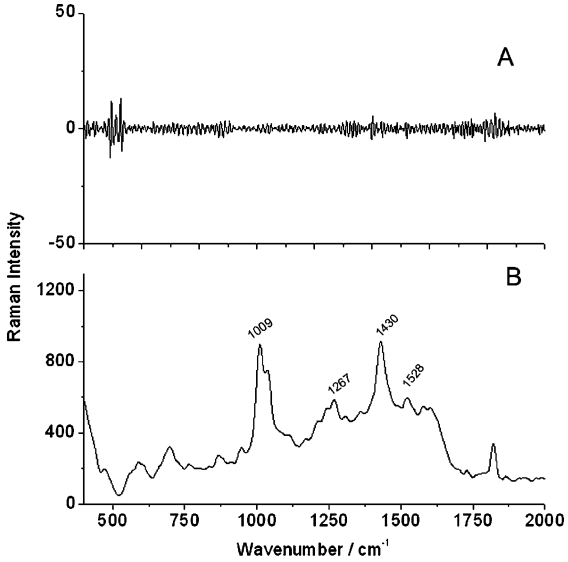

Figure 6. Raman spectra ($\lambda_{exc} = 785$ nm) of (A) a citrate-stabilized gold nanoparticle solution and (B) after inducing aggregation by the addition of an excess of potassium chloride.

promoted by the 2MPy ligand, and arises from the exciton coupling of nanoparticles in the aggregates.

In Figure 6 are shown the Raman spectra of gold nanoparticles stabilized by citrate. At the excitation wavelength of 785 nm, there was no evidence of Raman peaks, indicating a negligible SERS effect (Figure 6A). However, by the addition of a concentrated solution of potassium chloride, the stability of the modified gold nanoparticles is reduced because of the increase of the ionic strength. The resulting aggregation enhances the SERS effect, allowing the observation of the citrate ion vibrational peaks in the Raman spectra (Figure 6B) at 1009, 1267, 1430, and 1528 cm^{-1} ascribed to ν(CC), ν_a(OCO), ν_s(COO), and ν_{as}(COO), respectively, by analogy with the spectra of citrate-modified silver nanoparticles.[13] The split between the signal positions of ν_s(COO) and ν_{as}(COO) is sensitive to the mode of surface coordination of the carboxylate group.[14] The observed split of 98 cm^{-1} indicates that the carboxylate groups of citrate anions are coordinating to the gold atoms in a bidentate manner.

According to the electromagnetic theory of SERS,[15] when the particles are much smaller than the exciting wavelength, the enhancement G is given by eq 6, where i refers to the

$$G = \left| i + \frac{\alpha^3 g_0[3\mathbf{n}(\mathbf{n}\cdot i) - i]}{\mathbf{r}'^3} + \frac{\alpha^3}{\mathbf{r}'^3} g\left\{\left(\frac{\alpha^3 g_0}{\mathbf{r}'^3} - 1\right) i + \left(\frac{\alpha^3 g_0}{\mathbf{r}'^3} + 1\right)[3\mathbf{n}(\mathbf{n}\cdot i)]\right\}\right|^2 \quad (6)$$

polarization of the incident field at $\mathbf{r}'$ [i.e., $E(\mathbf{r}',\omega_0) = E_0\mathbf{i}$], $\mathbf{n} = \mathbf{r}'/r'$, a is the radius of the particle, and g and g_0 are the values of the function $(\epsilon - 1)/(\epsilon + 1)$, involving the refractive index of the material comprising the particle and that of the environment.

In the situation where the molecule is as close as possible to the particle ($r' = a$) and the polarization of the incident and scattered wave is perpendicular to the scattering plane, the enhancement factor is given by

$$G = 5[1 + 2g_0 + 2g + 4gg_0]^2 \quad (7)$$

According to eq 7, the maximum enhancement is obtained when $\epsilon' = -2\epsilon_m$, where ϵ' is the real part of the complex refractive index and ϵ_m is the medium refractive index.

Alternatively, from Mie's theory of scattering, it can be seen that the measured absorbance over a path length d is proportional to the extinction cross section C_{ext}:

$$A = NC_{ext}d/2.303 \quad (8)$$

where N is the number of noninteracting particles per unit of volume.[15] The extinction cross section for small and dilute nanoparticles is given by the relation

$$C_{ext} = 24\pi^2 a^3 \epsilon_m^{3/2} \epsilon''(\omega)/\lambda\{[\epsilon'(\omega) + 2\epsilon_m]^2 + \epsilon''(\omega)\} \quad (9)$$

where ϵ' is the real part of the complex refractive index, ϵ_m is the medium refractive index, and ϵ'' is the imaginary part of the complex dielectric function, which is related to the absorption coefficient. The maximum absorbance is obtained when $\epsilon' = -2\epsilon_m$, thus predominating the imaginary ϵ'' term in the denominator of the above equation. This is the resonance condition for plasmon excitation and for the occurrence of the maximum SERS intensification, according to the electromagnetic theory (eq 7).

As observed by Wang et al.,[16] not only should the orientation of the molecules near the particle surface be taken into consideration in the SERS effect but also the resonance condition between the nanoparticle and the incident radiation. Thus, the fact that small monodispersed nanoparticles exhibited no SERS effect (Figure 6A), while the aggregates exhibited strong enhancement of the Raman spectra, can be understood because the incident radiation of 785 nm is closer to the aggregate multipole excitation at 650 nm than to the surface plasmon band at 520 nm.

In the same way, by the addition of 2Mpy to citrate-stabilized gold nanoparticles, the pronounced aggregation in aqueous solution led to the SERS effect, enhancing the vibrational peaks of the adsorbed MPy ligand (Figure 7A). The SERS profile is dominated by the strong signals of the in-plane vibrational modes of 2MPy, β_{CH} and $\nu_{C=C/C=N}$, from 1200 to 1550 cm^{-1} and ring-breathing modes in the 1001−1116-cm^{-1} region. It should be noticed that the interaction of 2MPy with gold nanoparticles isolated in solid form has already been investigated by FTIR spectroscopy, involving the S atom of the adsorbed molecules.[1] On the other hand, according to the theoretical simulation of the vibrational spectra,[1] the adsorbed 2MPy molecule behaves as expected for the thiol form rather than for the thione one.

(13) Tada, H.; Bronkema, J.; Bell, A. T. *Catal. Lett.* **2004**, *92*, 93.
(14) Nakamoto, K. *Infrared and Raman Spectra of Inorganic and Coordination Compounds*, 4th ed.; John Wiley & Sons: New York, 1986.
(15) Moskovitis, M. *Rev. Mod. Phys.* **1985**, *57*, 783.
(16) Wang, Z.; Rothberg, L. J. *J. Phys. Chem. B* **2005**, *109*, 3387.

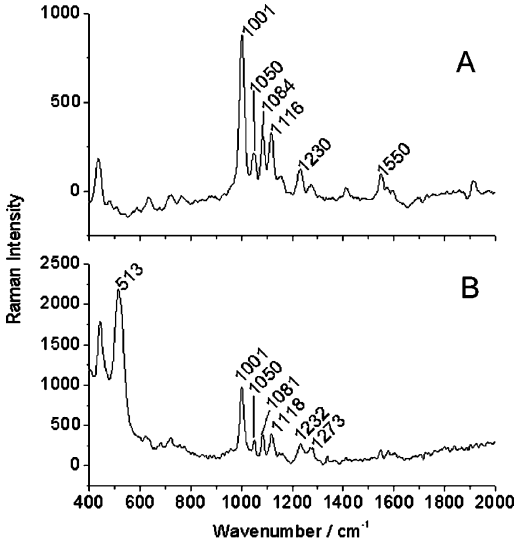

Figure 7. SERS profile of gold nanoparticles after inducing aggregation with (A) 2MPy and (B) $[Fe^{II}(CN)_5(2MPy)]^{3-}$ (both 3×10^{-4} mol dm^{-3}).

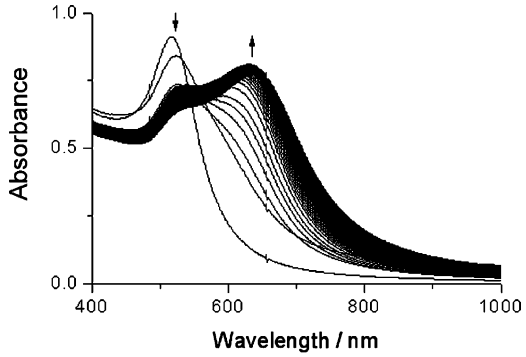

Figure 8. Successive spectra (time interval = 120 s) of a citrate-stabilized gold nanoparticle solution, after the addition of $[Fe^{II}(CN)_5(2MPy)]^{3-}$ (5×10^{-6} mol dm^{-3}).

By the addition of $[Fe(CN)_5(2MPy)]^{3-}$ to a citrate-stabilized solution of gold nanoparticles, the observed effect was quite similar to those induced by the 2MPy ligand alone, as one can see in Figure 8, showing a decrease of the 520-nm band in parallel with the rise of the 640-nm band. The corresponding Raman spectrum (Figure 7B) is similar to that observed for the gold nanoparticles in the presence of 2MPy. Therefore, the $[Fe(CN)_5(2MPy)]^{3-}$ complex should be acting as a source, delivering 2MPy to the gold nanoparticles. In addition, the presence of the new peak at 531 cm^{-1} ascribed to ν(Fe−CN)[17] is indicative of a parallel interaction but, to a small extent, of the gold nanoparticles with the remaining $[Fe(CN)_5(2MPy)]^{3-}$ species, via the CN bond.

In the case of 4MPy, the interaction with gold nanoparticles led to their immediate aggregation, precipitating after a few hours. In contrast with the gold−2MPy solid, which can be dissolved in methanol, the gold−4MPy precipitate has been reported[1] to be virtually insoluble in the conventional solvents.

The spectral changes produced by the addition of 4MPy to citrate-stabilized gold nanoparticles can be seen in Figure 9.

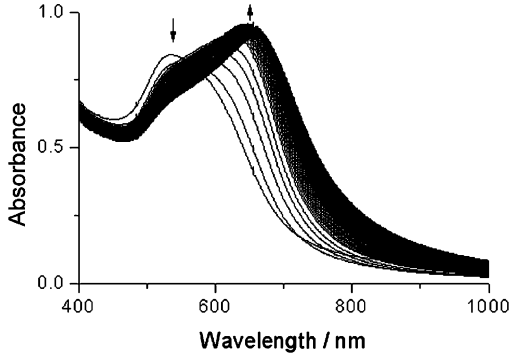

Figure 9. Successive spectra (time interval = 120 s) of a citrate-stabilized gold nanoparticles solution, after the addition of 4MPy (5×10^{-6} mol dm^{-3}).

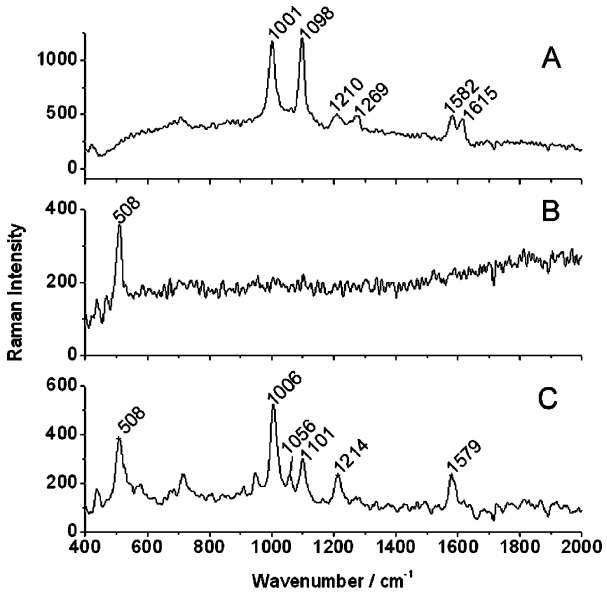

Figure 10. SERS profile of gold nanoparticles (A) after inducing aggregation with 4MPy, (B) after stabilization with $[Fe^{II}(CN)_5(4MPy)]^{3-}$ (both at 3×10^{-4} mol dm^{-3}), and (C) after inducing aggregation of $[Fe^{II}(CN)_5(4MPy)]^{3-}$-coated nanoparticles by the addition of an excess of potassium chloride.

The corresponding SERS profile can be seen in Figure 10A. One can note that the number of vibrational peaks of 4MPy is rather small, as compared with 2MPy, showing the ν(C−S) vibrational peak[2] at 1098 cm^{-1} and the ring-breathing mode at 1001 cm^{-1}, in addition to the $\nu_{C=C/C=N}$ peaks at 1582 and 1615 cm^{-1}. This result suggests a higher molecular symmetry, consistent with the perpendicular orientation of the 4MPy molecules with respect to the nanoparticle surface.[16,18] Such binding geometry would also facilitate the interaction of 4MPy with the neighboring particles by acting as a bridging ligand, giving rise to extended 3D aggregates.

In contrast, the addition of $[Fe(CN)_5(4MPy)]^{3-}$ to the gold nanoparticles leads their strong stabilization in aqueous solution, precluding the formation of aggregates, because of the high negatively charged coating, as one can see in Figure 11.

As observed for the citrate-stabilized gold nanoparticles, the small scattering cross section leads to a negligible SERS effect (Figure 10B) at λ_{ex} = 785 nm, except for the ν(Fe−

(17) Loo, B. H.; Lee, Y. G.; Liang, E. J.; Kiefer, W. *Chem. Phys. Lett.* **1998**, *297*, 83.

(18) Hu. J.; Zhao, B.; Xu, W.; Li, B.; Fan, Y. *Spectrochim. Acta, Part A* **2002**, *58*, 2827.

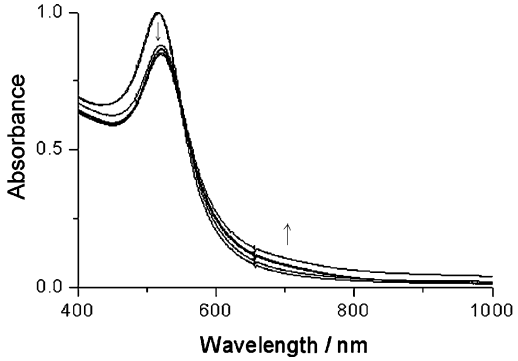

Figure 11. Successive spectra of a citrate-stabilized gold nanoparticles solution after the addition of a $[Fe(CN)_5(4MPy)]^{3-}$ solution (5×10^{-6} mol dm^{-3}).

CN) peak at 508 cm^{-1} indicative of a parallel binding mode, via the CN bond.[15] However, by the addition of a concentrated solution of potassium chloride in order to break the stability of the nanoparticles, the occurrence of aggregation gives rise to a strong SERS effect (Figure 10C). The enhanced vibrational peaks differ from those observed for the adsorbed 4MPy ligand, showing the ν(CS) vibrational peak at 1101 cm^{-1} and the ring-breathing vibrations at 1006 and 1056 cm^{-1}, in addition to the $\nu_{C=C/C=N}$ peaks at 1579 cm^{-1}, indicating that the $[Fe(CN)_5(4MPy)]^{3-}$ complex is anchored on the gold nanoparticles mainly via the S atom. The parallel binding mode via the CN bond is also observed from the ν(Fe−CN) peak at 508 cm^{-1} and the ν(CN) peaks at 2129 and 2161 cm^{-1} (not shown).

Aggregation Kinetics. The addition of 2MPy, 4MPy, or $[Fe(CN)_5(2MPy)]^{3-}$ to the citrate-stabilized gold nanoparticles led to a rapid decrease of the intensity of the 520-nm plasmon band due to the binding of the thiols and to the rise of a broad band around 650 nm, as depicted in Figures 5, 8, and 9, associated with the formation of aggregates. The kinetics behavior monitored at the two wavelengths exhibited the time dependence shown in Figure 12, approaching the end point in a few seconds.

Titration experiments have shown that initially the aggregated and nonaggregated nanoparticles coexist in equilibrium. By variation of the concentration of the MPy's, from 6×10^{-7} to 5×10^{-6} mol dm^{-3}, the maximum absorbance around 650 nm increased systematically, approaching a saturation behavior but without completely depleting the original band at 520 nm, even when the thiol is added in greater excess. The presence of a residual plasmon band around 520 nm indicates that electronic coupling is not so effective in the aggregates, thus preserving to a small extent the characteristics of the original nanoparticles.

Recently, an interesting study on the kinetics of citrate-stabilized gold nanoparticles and the negatively charged 3-mercapto-1-propanesulfonate, or positively charged 2-mercaptoethylammonium species, has been carried out by Calvo et al.[19] According to this study, the binding (adsorption) of negatively charged thiols can be the rate-determining step, proceeding relatively slowly at the beginning because of the

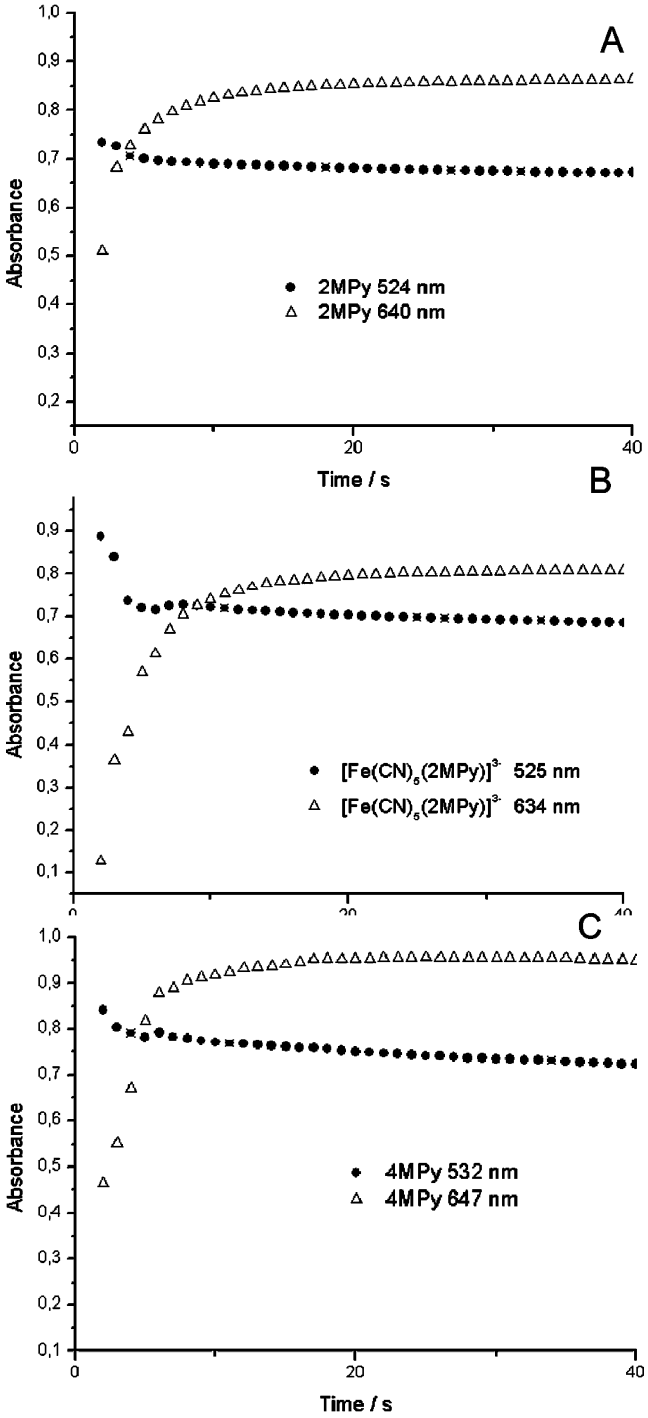

Figure 12. Time decay of the plasmon band around 520 nm of citrate-stabilized gold nanoparticles and aggregation (650 nm), after the addition of (A) 2MPy, (B) $[Fe(CN)_5(2MPy)]^{3-}$, (C) 4MPy solutions, in a concentration of 5×10^{-6} mol cm^{-3}.

electrostatic repulsion with the negatively charged nanoparticle, with a subsequent acceleration as the citrate shell is gradually replaced. In our case, the thiol ligands are in the neutral form and the binding process seems to be rather fast, as shown by the rapid initial decay of the 520-nm band, preceding the aggregation kinetics responsible for the rise of the 650-nm band.

Conclusion

Multifunctional sulfur-containing ligands such as 2MPy and 4MPy and their corresponding pentacyanoferrate(II)

(19) Bellino, M. G.; Calvo, E. J.; Gordillo, G. *Phys. Chem. Chem. Phys.* **2004**, *6*, 424.

complexes can interact with gold nanoparticles through the S atom, providing different modes of stabilization or aggregation in aqueous solution. 2MPy form aggregates exhibiting the SERS effect for typical vibrational modes of the molecule while shifting the gold plasmon band to 640 nm. The corresponding S-coordinated $[Fe(CN)_5(2MPy)]^{3-}$ complex is not able to stabilize the gold nanoparticles. Because of its intrinsic lability, it helps in delivering the 2MPy ligand to the gold nanoparticles, promoting their aggregation. 4MPy also induces the aggregation of the gold nanoparticles, yielding rather insoluble products, involving cross-linking between the neighboring particles. In contrast, the N-coordinated $[Fe(CN)_5(4MPy)]^{3-}$ complex can strongly bind the gold nanoparticles, preventing their aggregation in aqueous solution.

Acknowledgment. The support from FAPESP, CNPq, IM2C, and RENAMI is gratefully acknowledged.

IC0512429